Microscopic Measurement of the Pair Interaction Potential of Charge-Stabilized Colloid

John C. Crocker and David G. Grier
The James Franck Institute, The University of Chicago, 5640 South Ellis Avenue, Chicago, Illinois 60637
(Received 14 January 1994)

We present a microscopic measurement of the interaction potential between isolated pairs of charged colloidal spheres. The measured spatial dependence of the potential is consistent with the screened Coulomb repulsion expected from the Derjaguin-Landau-Verwey-Overbeek theory of colloidal interactions.

PACS numbers: 82.70.Dd

The past century of research on charge-stabilized colloidal suspensions has been inspired by their intrinsic interest as distinct states of matter [1], by their considerable technological value [2], and more recently by their utility as model condensed matter systems [3,4]. The standard theory for the interaction between charged colloidal spheres was formulated almost 50 years ago by Derjaguin-Landau-Verwey-Overbeek (DLVO) [5,6]. Calculations based on the DLVO theory [7–9] account at least qualitatively for the observed fluid-crystal and fcc-bcc phase boundaries [10,11] as well as for many of these phases' bulk properties [12,13]. Persistent quantitative discrepancies [10,11] and anomalous observations including the unaccounted for monodisperse glassy phase [11] suggest that the theory is not yet complete, however. Differences with the DLVO theory also have been raised on theoretical grounds [14–18]. In light of the fundamental importance of these considerations to the understanding of colloidal systems, we have measured the colloidal pair potential directly, utilizing digital video microscopy and optical trapping techniques. In particular, we extract the two-particle interaction from the dynamics of isolated pairs of particles moving away from artificially created initial configurations.

The colloid in our study consists of commercially available polystyrene sulfate spheres with radius $a=32$ nm, monodisperse to within 1% (Duke Scientific, No. 5065A). Particles of this size undergo vigorous Brownian motion in water and yet are sufficiently large to be imaged with a conventional light microscope. When such spheres are dispersed in water, the ionic groups bonded to their surfaces dissociate and give rise to a screened electrostatic interaction. For sphere separations large enough that the Debye-Hückel approximation holds, the DLVO theory gives the potential:

$$U_{\mathrm{DLVO}}(x)=\frac{Z^{*2}e^2}{\varepsilon}\left[\frac{e^{2\kappa a}}{(1+\kappa a)^2}\right]\frac{e^{-\kappa x}}{x}. \qquad (1)$$

Here x is the center-to-center distance between identical spheres, Z^* is their effective surface charge, ε is the dielectric constant of the solution, and κ^{-1} is its Debye-Hückel screening length set by the counterion concentration. Nonlinear contributions near the spheres' surfaces cause the effective surface charge to be considerably smaller than the fully dissociated surface charge. The spheres in our study, for example, have titratable charges of $(3.2\pm0.5)\times10^5$ electron equivalents although their effective surface charge, Z^*, is more than 2 orders of magnitude smaller, as we will see below. For such highly charged spheres, the screened Coulomb interaction dominates van der Waals and hydrodynamic contributions which therefore do not appear in Eq. (1).

The possibility has been raised that a more comprehensive treatment of the counterion free energy might reveal a long-range attractive component [14–18] to the interaction potential. Such attractive regimes are known to occur in the parallel plate geometry [19]. Strong long-range attraction would account for such experimental observations as phase separation in monodisperse colloidal fluids [20,21] and stable multiparticle voids in colloidal crystals.

The majority of previous tests of the DLVO theory have relied on indirect probes such as elastic constant and phase boundary measurements. The calculated values for these bulk properties, however, are quite insensitive to the form of the local interaction potential, and the measurements also may reflect many-body contributions. Inversion of light scattering data is notoriously sensitive to noise and requires the assumption of a functional form for the potential [22]. The second virial coefficient of dilute suspensions extracted from light scattering data similarly relies for its interpretation on a model for the interaction [23]. The pioneering work of Takamura, Goldsmith, and Mason [24] sought the microscopic interaction's spatial dependence in the dynamics of particle pairs colliding in a shear flow. Deviations from paths predicted for noninteracting spheres provided estimates for parameters in their interaction model. Since their method relies on hydrodynamic calculations, it is applicable only in the absence of Brownian motion. Furthermore, as we will see below, the scale of forces which characterizes long-range colloidal interactions is small enough to challenge even atomic force microscopes. The method of the present study requires no assumptions for the form of the interaction beyond spherical symmetry, explicitly excludes many-body contributions, can probe weakly interacting systems with strong Brownian motion, and thus addresses colloidal systems of the greatest theoretical and practical interest.

0031-9007/94/73(2)/352(4)$06.00

Unlike indirect probes of the potential, particle trajectories exactly represent their progenitor forces. However, extracting the pair potential from an enormous background of random thermal forces requires some care. Assuming the colloidal interaction is spherically symmetric, we cast the analysis into a one-dimensional form by considering only the particles' relative coordinate. This is conceptually equivalent to studying the dynamics of one particle (with correspondingly larger Brownian motion) moving in the potential $U(x)$ set up by another stationary particle. The probability density, $\rho(x,t)$, for finding a particle as it diffuses through a viscous fluid in a one-dimensional static potential, $U(x)$, satisfies the Smoluchowski equation [25],

$$\frac{\partial\rho(x,t)}{\partial t} = L_S\rho(x,t)\,, \tag{2}$$

where

$$L_S = \left[\frac{1}{m\gamma}\frac{\partial}{\partial x}U'(x) + \frac{k_BT}{m\gamma}\frac{\partial^2}{\partial x^2}\right]. \tag{3}$$

$U'(x)$ denotes the spatial derivative of $U(x)$ and $\gamma = 6\pi\eta a$ is the Stokes drag coefficient for a particle of mass m and radius a moving through a fluid of viscosity η. The probability density satisfying the Smoluchowski equation evolves in time according to

$$\rho(x,t+\tau) = \int P(x,t+\tau|x',t)\rho(x',t)dx'\,, \tag{4}$$

where

$$P(x,t+\tau|x',t) = e^{L_S\tau}\delta(x-x')\,. \tag{5}$$

Because the operator L_S does not include hydrodynamic coupling and $U(x)$ depends only on the instantaneous separation, the propagator, $P(x,t+\tau|x',t)$, depends only on the propagation time τ and not on t. The history independence of the propagator permits us to select as the propagation time $\tau = 1/30$ sec, the delay between consecutive video frames.

The equilibrium probability density, $\rho^{eq}(x)$, is the stationary solution of Eq. (4). Discretizing the spatial dependence in Eq. (4) then yields

$$\rho_i^{eq} = \sum_j P_{ij}\rho_j^{eq}\,, \tag{6}$$

where ρ_i^{eq} is the probability of finding the particle in the ith spatial bin and P_{ij} is the discrete approximation to the continuous transition probability, $P(x,\tau|x',0)$. Because the equilibrium probability density is related to the interaction potential through the Boltzmann distribution, $\rho_i^{eq} = \exp[-U(x_i)/k_BT]$, the experimental problem of determining the interaction potential is reduced to characterizing the transition probability matrix, P_{ij}.

The experimental arrangement is rendered in Fig. 1(a). We strove to minimize the concentration of ionic impurities and thereby maximize the range of the colloidal interaction. Our cell was constructed by hermetically sealing the edges of a No. 1 microscope cover slip (150 μm thick) to the surface of a standard microscope slide. Holes drilled through the slide connect the thin sample volume to reservoir tubes filled with mixed-bed ion exchange resin. All glass surfaces were cleaned thoroughly before assembly. After filling with de-ionized colloidal suspension, the reservoir tubes are continuously flushed with water-saturated argon at a small overpressure to prevent contamination by airborne CO_2. Regulating the gas pressure in the reservoir tubes allows us to adjust the separation between slide and cover slip with submicron precision. When such a cell was filled with a dense suspension (volume fraction $\phi = 0.04$–0.05), colloidal crystals with fcc ordering formed rapidly and were observed to persist for months, indicating that such cells can remain relatively free of ionic impurities for long periods.

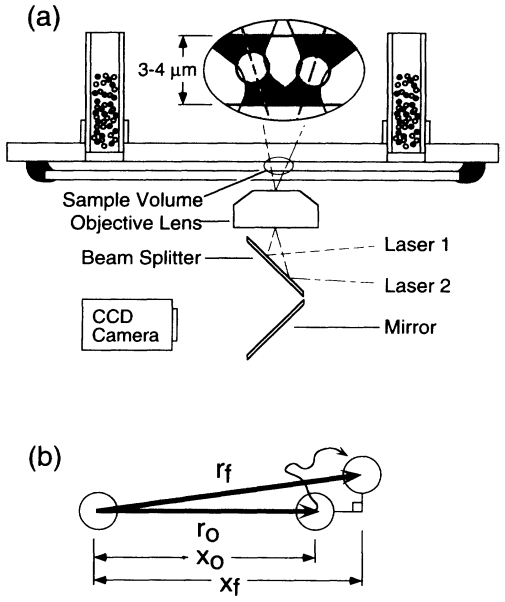

FIG. 1. (a) Schematic representation of the sample cell in cross section. The reservoir tubes are connected to gas transfer systems which are omitted for clarity. The inset shows a magnified view (not to scale) of two colloidal spheres trapped in a pair of optical tweezers between the glass walls of the sample cell. (b) Projection of the one-dimensional separations, x_0 and x_f.

To perform interaction measurements, the cell is filled with a dilute suspension and mounted on an inverted (bright field) optical microscope with an attached video camera. We use a 100× numerical aperture 1.2 oil immersion objective and a total system magnification of 115 nm per pixel on our CCD camera. Two particles, selected at random, are held at a fixed separation (either 1.5 or 1.7 μm) with dual optical tweezers projected into the cell through the microscope objective [26,27]. The objective lens forms the tweezers by tightly focusing two laser beams, each of which localizes a dielectric sphere in three dimensions with optical gradient forces. A single 15 mW

argon-ion laser operating at a wavelength of 488 nm provides enough power to form both traps. We release the spheres by interrupting the laser beam when no other particles are near. Their subsequent motions are captured with a computer-controlled SVHS video deck (NEC PC/VCR). In all, the dynamics of 796 pairs of spheres were recorded in this manner. Weak absorption of laser light at the experimental wavelength coupled with rapid thermal conduction by the water limit temperature increases in the trapped particles to less than 0.1 K. This small degree of heating will not measurably alter the interaction between the spheres. Thermal conduction also dissipates temperature gradients across the sample volume with a characteristic time shorter than 1 μsec.

Several steps are required to extract P_{ij} from the videotaped trajectories. First, the video tape is digitized with a precision frame grabber (Data Translation DT-3851A). The images are then corrected for geometric distortion and spatially filtered to suppress variations in illumination and camera noise. An individual sphere appears in an image as a maximum in the local brightness field. We refine its location to better than 25 nm (about 1/5 pixel) in the focal x-y plane by calculating the brightness-weighted centroid of the pixels it subtends. Because motion out of the focal plane (in the z direction) changes a sphere's appearance, its z coordinate can be estimated to within 150 nm by calibrating its apparent brightness and size as functions of its depth. Since the particles' separation vector lies approximately in the x-y plane, the measurement error in z adds only in quadrature; the mean error in the separation measurement is estimated to be 50 nm.

A single video frame is composed of two fields containing odd- and even-numbered lines, respectively, which are acquired 1/60 sec apart. We locate spheres in each video field separately to avoid location error due to their motion between fields. Having located a sphere in one video frame, its identification in subsequent frames is estimated with a maximum likelihood algorithm. To avoid possible systematic errors, we measure displacements between even fields and odd fields separately. The propagation time is still 1/30 sec and the four fields from two frames provide two independent samples of the particles motion. Details of the image processing and analysis will be presented elsewhere.

In consecutive video frames, a pair of spheres evolves from an initial vector separation, $\mathbf{r}_0$, to a final separation, $\mathbf{r}_f$. There are more ways for a pair of noninteracting spheres to wander apart than to come together in two or more dimensions. To avoid the resulting bias in our data set, we project the final separation vector onto the direction of the initial separation vector, as shown in Fig. 1(b). The transverse motion in one time step is sufficiently smaller than the center-to-center separation that the resulting error is smaller than our spatial resolution. Our data set also could be biased in the opposite direction if we were to consider the initial conditions too close to either wall. In this case, the walls can prevent particles from wandering apart. To avoid this bias we restrict our data set to those trajectory steps with initial positions no further from the cell's midplane than $2\sqrt{2D\tau}=422$ nm, where the self-diffusion coefficient $D=0.67$ μm^2/sec for spheres of radius $a=326$ nm.

Our 796 pair trajectories yield 6502 independent (x_0,x_f) samples of the transition probability. We distribute these measurements into the matrix elements of P_{ij} with weightings which are inversely proportional to the local density of initial separations. Weighting in this manner compensates for the nonuniform distribution of x_0 values. The bin size is half a pixel (57 nm). We approximate the errors $\delta\rho_i^{eq}$ in the elements of ρ_i^{eq} from the matrix δP_{ij} of standard deviations of P_{ij} as $(\delta\rho_i^{eq})^2=\sum(\delta P_{ij}\rho_j^{eq})^2$.

In practice, we limit the range of separations considered to a value x_{max}. Those measurements (x_0,x_f) with $x_0<x_{max}$ and $x_f>x_{max}$ are distributed into P_{ij} as $(x_0,2x_{max}-x_f)$. This reflecting boundary condition compensates for the tendency of ρ_i^{eq} to vanish under free diffusion. Provided that x_{max} is larger than the range of the interaction, our results do not depend on x_{max}.

The pair interaction potential measured in this manner appears in Fig. 2. The solid line is a two-parameter fit to Eq. (1) which yields an effective charge of $Z^*=1991\pm150$ electronic charges and a Debye-Hückel screening length of $\kappa^{-1}=161\pm10$ nm. This value is considerably smaller than the maximum screening length of 960 nm in pure water and is consistent with a $3.6\times10^{-6}M$ concentration of a 1:1 electrolyte. This estimate for the surface charge should be considered a lower limit because the interaction curve is broadened slightly by measurement errors in the spheres' locations. The qualitative agreement between our measurement and the DLVO theory is excellent with no statistically significant evidence of a long-

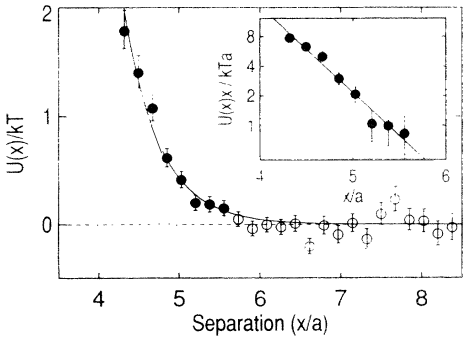

FIG. 2. Measured pair interaction potential for spheres of radius $a=0.326$ μm as a function of center-to-center separation. The solid curve is a fit to Eq. (1) with $Z^*=1991e$ and $\kappa^{-1}=161$ nm. Inset: Semilogarithmic plot of the filled data points together with corresponding fit line. The line's slope provides an estimate for the Debye-Hückel screening length.

range attractive interaction.

The estimated surface charge on our spheres is more than 2 orders of magnitude smaller than their titratable charge. Charge renormalization calculations [12] suggest that for very highly charged colloid the effective charge should saturate at $Z^* = C(a/\lambda_B)$, where the Bjerrum length is $\lambda_B = z^2e^2/\varepsilon k_B T = 0.715$ nm for a 1:1 electrolyte in water at 25 °C, and C is a constant around 10. A molecular dynamics simulation [28] of a spherically symmetric charged colloidal system finds $C = 7$ in reasonable agreement with measurements on micelles [29] which find $C = 6$. Our measured charge of $Z^* = 1991$ corresponds to $C = 4.4$.

While the present study has focused on a system with fairly large screening length and high surface charge, our technique also should apply to systems with weaker interactions. Such measurements hold the promise of systematizing the study of colloidal phases and their properties. It is noteworthy that the present measurements correspond to a force resolution on the order of 10^{-15} N. Our method should prove complementary to two other new techniques: That of Calderon *et al.* measures the highly energetic interactions of monodisperse systems driven into linear chains by external fields [30], and the direct imaging technique of Fraden derives information from extensive statistics on the instantaneous distribution of thermally equilibrated systems [31]. The relative simplicity and versatility of our technique suggests several immediate applications. Measurements of the effective charge as a function of temperature, sphere size, and dielectric constant will facilitate refinement of the charge renormalization theory. We can also test the linearity of the interaction by studying spheres with unequal radii. Such measurements will be crucial in understanding the bulk properties of bidisperse systems.

We would like to thank C. Murray, T. Witten, L. Kadanoff, M. Robbins, D. Weitz, and S. Fraden for valuable insights. This work was supported by the NSF Materials Research Laboratory at The University of Chicago through Grant No. DMR88-19860. Additional funding was provided by DOE.

[1] W. B. Russel, D. A. Saville, and W. R. Schowalter, *Colloidal Dispersons* (Cambridge University Press, Cambridge, 1989).

[2] P. A. Rundquist, P. Photinos, S. Jagannathan, and S. A. Asher, J. Chem. Phys. **91**, 4932 (1989).

[3] P. Pieranski, L. Strzlecki, and B. Pansu, Phys. Rev. Lett. **50**, 900 (1983).

[4] C. A. Murray, in *Bond-Orientational Order in Condensed Matter Systems*, edited by K. J. Strandburg (Springer-Verlag, Berlin, 1991).

[5] B. V. Derjaguin and L. Landau, Acta Physicochimica (USSR) **14**, 633 (1941).

[6] E. J. Verwey and J. T. G. Overbeek, *Theory of the Stability of Lyophobic Colloids* (Elsevier, Amsterdam, 1948).

[7] P. M. Chaikin, P. Pincus, S. Alexander, and D. Hone, J. Colloid Interface Sci. **89**, 555 (1982).

[8] D. Hone, S. Alexander, P. M. Chaikin, and P. Pincus, J. Chem. Phys. **79**, 1474 (1983).

[9] M. O. Robbins, K. Kremer, and G. S. Grest, J. Chem. Phys. **88**, 3286 (1988).

[10] Y. Monovoukas and A. P. Gast, J. Colloid Interface Sci. **128**, 533 (1989).

[11] E. B. Sirota, H. D. Ou-Yang, S. K. Sinha, P. M. Chaikin, J. D. Axe, and Y. Fujii, Phys. Rev. Lett. **62**, 1524 (1989).

[12] S. Alexander, P. M. Chaikin, P. Grant, G. J. Morales, P. Pincus, and D. Hone, J. Chem. Phys. **80**, 5776 (1984).

[13] H. M. Lindsay and P. M. Chaikin, J. Chem. Phys. **76**, 3774 (1982), and references therein.

[14] I. Sogami, Phys. Lett. **96A**, 199 (1983).

[15] I. Sogami and N. Ise, J. Chem. Phys. **81**, 6320 (1984).

[16] L. Guldbrand, B. Jönsson, H. Wennerström, and P. Linse, J. Chem. Phys. **80**, 2221 (1983).

[17] C. E. Woodward, J. Chem. Phys. **89**, 5140 (1988).

[18] C. E. Woodward, B. Jönsson, and T. Åkesson, J. Chem. Phys. **89**, 5145 (1988).

[19] J. Israelachvili, *Intermolecular and Surface Forces* (Academic, London, 1992).

[20] T. Okubo, J. Chem. Phys. **90**, 2408 (1989).

[21] B. V. R. Tata, M. Rajalakshmi, and A. K. Arora, Phys. Rev. Lett. **69**, 3778 (1992).

[22] R. Rajagopalan, in *The Structure, Dynamics, and Equilibrium Properties of Colloidal Systems*, edited by D. M. Bloor and E. Wyn-Jones (Kluwer Academic, Boston, 1990), p. 695.

[23] M. L. Gee, P. Tong, J. N. Israelachvili, and T. A. Witten, J. Chem. Phys. **93**, 6057 (1990).

[24] K. Takamura, H. L. Goldsmith, and S. G. Mason, J. Colloid Interface Sci. **82**, 175 (1981).

[25] H. Risken, *The Fokker-Planck Equation* (Springer-Verlag, Berlin, 1989).

[26] R. S. Afzal and E. B. Treacy, Rev. Sci. Instrum. **63**, 2157 (1992).

[27] A. Ashkin, J. M. Dziedzic, J. E. Bjorkholm, and S. Chu, Opt. Lett. **11**, 288 (1986).

[28] M. Robbins (private communication).

[29] S. Bucci, C. Fagotti, V. Degiorgio, and R. Piazza, Langmuir **7**, 824 (1991).

[30] F. L. Calderon, T. Stora, O. M. Monval, P. Poulin, and J. Bibette (to be published).

[31] S. Fraden (private communication).

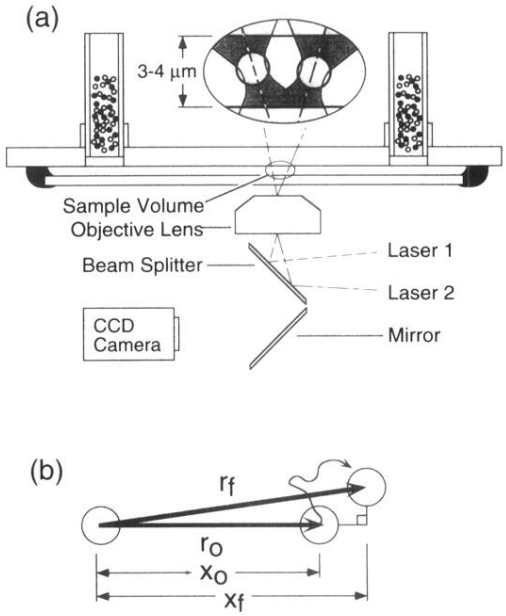

FIG. 1. (a) Schematic representation of the sample cell in cross section. The reservoir tubes are connected to gas transfer systems which are omitted for clarity. The inset shows a magnified view (not to scale) of two colloidal spheres trapped in a pair of optical tweezers between the glass walls of the sample cell. (b) Projection of the one-dimensional separations, x_0 and x_f.